VIBRATION AND ECCENTRICITY MEASUREMENTS COMBINED WITH ROTORDYNAMIC ANALYSES ON A SIX BEARING TURBINE GENERATOR

by
David R. Gruwell
Senior Engineer
Public Service Company of New Hampshire
Manchester, New Hampshire
and
Fouad Y. Zeidan
President
Bearings Plus/KMC, Inc.
Houston, Texas

David R. Gruwell is Rotating Equipment Specialist at Public Service of New Hampshire, in Manchester. Before joining PSNH in 1980, he was employed by General Electric Company for 10 years. Seven of those years were in the Installation & Service Engineering Department, where he was promoted to Gas Turbine Specialist. At PSNH, Mr. Gruwell has been the project engineer for the retrofit of three steam turbine generator units with modern design LP turbines. He has applied non OEM tilt pad bearings to both HP and LP turbines to improve performance and to reduce the outage time required to fit and align bearings. He coauthored a paper, "Life Extension Strategies for Cracked Disk Attachments of Low Pressure Steam Turbines," for the 1994 International Joint Power Generation Conference.

Mr. Gruwell received his B.S. degree (Mechanical Engineering) from Iowa State University (1970), and is a registered Professional Engineer in the State of New Hampshire.

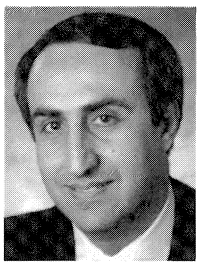

Fouad Y. Zeidan is the President of Bearings Plus/KMC, Inc., in Houston, Texas. He joined KMC in 1992 as Director of Engineering and became the V.P. of Engineering/General Manager in 1995. Prior to joining KMC, he held positions at Amoco Research Center, IMO Industries CentriMarc Division, and Qatar Fertilizer where he worked in engineering and maintenance of rotating and critical plant machinery. Dr. Zeidan holds seven U.S. Patents for integral squeeze film dampers, flexure pivot journal and thrust bearings, and other related products. He has published more than 30 technical papers and articles on various turbomachinery topics.

Dr. Zeidan received his B.S. (Mechanical Engineering, 1978), M.S. (Mechanical Engineering, 1979), and Ph.D. (1989) degrees from Texas A&M University. He is a member of ASME, STLE, and the Vibration Institute.

ABSTRACT

This lecture discusses how the vibration characteristics and eccentricity measurements were combined with rotordynamic analyses to help improve the reliability of a turbine generator unit. It also explains certain vibration characteristics at partial load conditions that resulted in changes of the bearing load magnitude and direction. The measurements of a stable backward whirl orbit at certain load conditions will be shown and discussed. The rotordynamic analyses also simulated field balancing measurements that compared well with the synchronous response calculations. These analyses were also used to examine the benefits of retrofitting a steady bearing at the unsupported shaft pump extension.

INTRODUCTION

The 120 MW turbine generator consisted of a high pressure intermediate pressure (HP IP) rotor, a low pressure (LP) rotor, and a generator rotor. This train is supported on six bearings as shown in the rotordynamic model in Figure 1. The #1 and #2 bearings were already retrofitted with tilt pad bearings, but the conversion was not satisfactory. The bearings ran hot, and changes to oil flow did not result in the desired improvements. Increasing the bearing clearance managed to drop the temperature slightly, but this seemed to come at the expense of high vibrations above 90 MW, due to the loss of bearing damping. The #1 bearing experienced severe vibrations in the 90 to 100 MW range. This was attributed to the effect introduced by the partial steam admission that resulted in the load direction being at 45 degrees from the vertical axis, directly in line with the pivot in a four pad load-between-pad bearing.

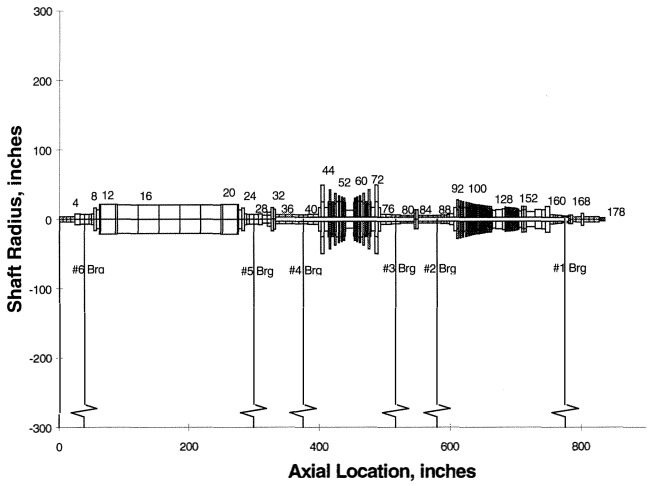

Figure 1. Rotor Model for 120 MW Turbine Generator.

Bearing and rotordynamic analyses investigations were performed in preparation for a major overhaul of the unit to improve efficiency and overall reliability. The objective of the analyses was to improve certain design features in the bearing configuration and to enhance the rotordynamic characteristics without causing any adverse effects. Vibration data were used to verify the computer model and provide a benchmark for the rotordynamic analyses predictions. The bearings had only one probe at each bearing location prior to the turnaround, making it difficult to measure shaft eccentricity and orbit for investigating the effect of side loads and partial steam admission. The additional probe was installed during the turnaround and provided very important information that helped in explaining the variation in the pad metal temperatures at certain operating conditions.

Gruwell and Zeidan (1997) showed the limitations with the existing bearings and need for design improvements. Photographs of the #1 four pad tilt pad bearing are shown in Figure 2 (a, b). The pads were supported on a relatively flexible ring (retainer), which in turn fitted in the annulus of the bearing housing shown in Figure 2 (c). Due to the limitation with this retainer, the floating seals could not be bolted to the retainer and had to be bolted to the bearing casing, which presented difficulties during assembly and inspection. The support was limited to a small area, which degraded the damping available in the fluid film.

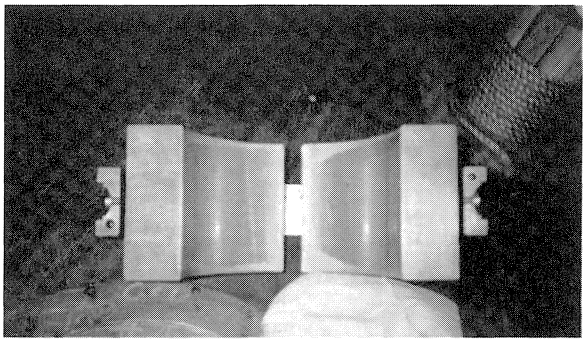

(a)

(b)

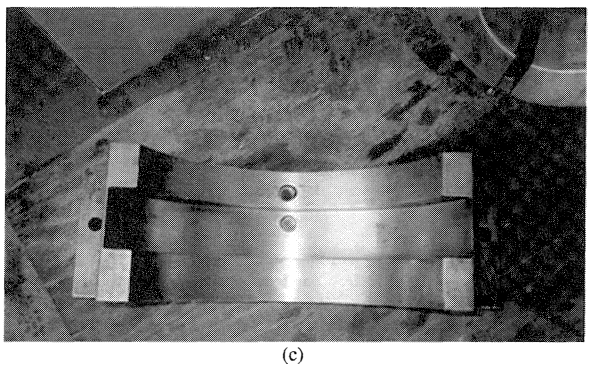

(c)

Figure 2. Existing #1 Tilt Pad Bearing.

The #2 tilt pad bearing had a spherical OD housing where the four spherical OD support/alignment pads rested. The bottom half of this housing is shown in Figure 3. The fit area for the alignment pads showed indications of severe fretting. While this spherical feature in the bearing alignment pads and housing was originally intended to allow the sleeve bearings to align to the shaft's catenary deflection curve, it was of no benefit in the case of tilting pad bearings that have the capability of axially aligning to the shaft. The #2 bearing had the floating seals bolted to the tilt pad retainer, but there was no provision to keep the bearing square to the shaft while it was being aligned and fitted within the spherical bore. This resulted in a very elaborate alignment and checking procedure to ensure that the seals were not wiped during startup.

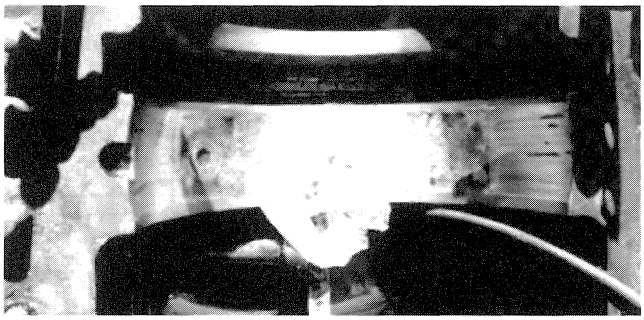

Figure 3. Spherical Housing for #2 Bearing.

ROTORDYNAMIC ANALYSIS AND BEARING OPTIMIZATION

An outage was planned for September/October 1996, to perform some rotor and stationary blading repair and to address the bearing problems, thus improving the overall reliability and efficiency of the unit. The objective of the bearing optimization and conversion was to provide a better design by investigating the use of a five pad or six pad bearing at the #1 bearing location. This was done in order to reduce the sensitivity to partial steam admission conditions through the use of a shorter pad arcs (stiffer pads). The objective was also to have a better bearing retainer and oil end seal design, and to eliminate the spherical fit on the #2 bearing. The plant planned to set up a boring bar to modify the spherical fit on the #3 bearing. These tools were used to cut the spherical fit on the #2 bearing into a cylindrical fit.

Rotor Model Verification

The rotor was modelled using Murphy's (1996-1998) XLROTOR rotordynamic program, which is based on the polynomial transfer matrix method. Due to the possibility for numerical errors that may result when the transfer matrix programs are used to model relatively long flexible rotors with many bearings, a verification of the program had to be performed prior to commencing with the analysis. The rotor was modelled from right to left and from left to right, as shown in Figures 1 and 4. The agreement in the analysis results with either model verified the adequacy of the program to handle this relatively large model.

Vibration data were then used to benchmark the model and verify the location of the peak responses (critical speeds). The vibration data shown in Figures 5 and 6, taken on March 24, 1995, revealed that the first HP IP rotor critical speed falls between 1600 and 1750 rpm. Figures 7 and 8 show the transient data taken on May 6, 1996, just prior to the outage. These data indicated some degradation in the vibration characteristics, as evident by the higher vibration levels when traversing the critical speed.

The rotordynamic analysis, shown in Figure 9, confirmed the validity of the model, as evident by the ability to closely predict the location of the critical speeds. Once the rotor model was verified, the bearing optimization was carried out to determine the best bearing configuration at the #1 and #2 bearing locations.

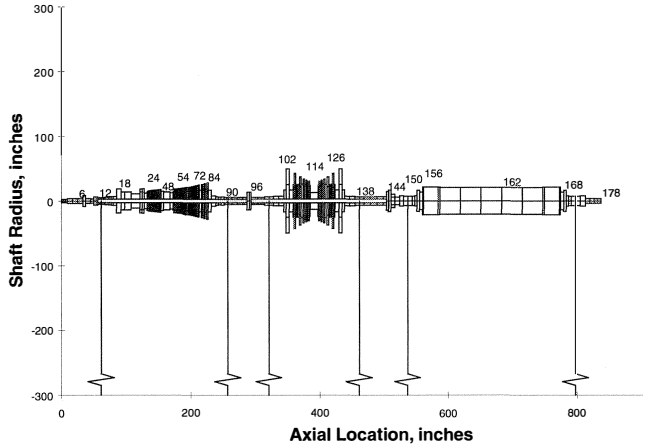

Figure 4. Turbine Generator Rotor Modelled from Left to Right.

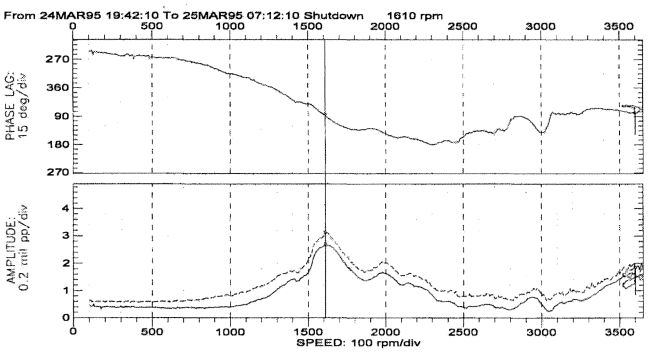

Figure 5. Coastdown Data at #1 Bearing Location.

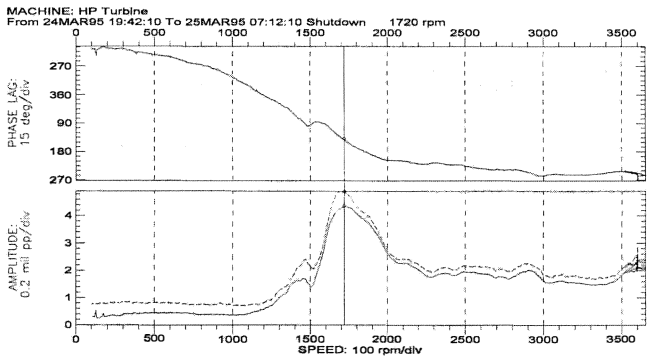

Figure 6. Coastdown Data at #2 Bearing Location.

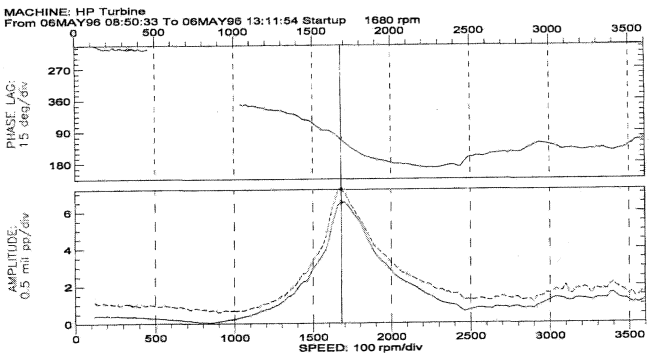

Figure 7. Startup Data at #1 Bearing Location.

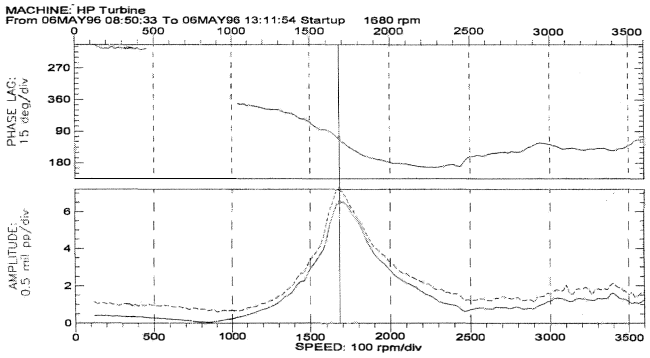

Figure 8. Startup Data at #2 Bearing Location.

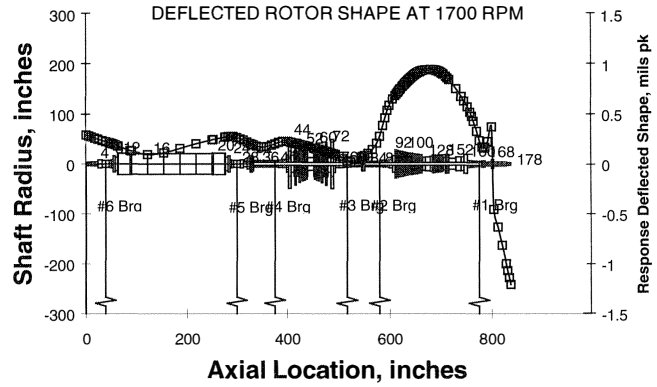

Figure 9. Deflected Rotor Shape at Critical Speed.

Bearing Optimization

Bearing optimization was carried out by simulating different bearing configurations at the #1 and #2 locations. In the case of the #1 bearing, five pad and six pad bearings were analyzed, where the geometric preload and pivot offset were investigated. In the case of the #2 bearing, only a four pad bearing was analyzed, but with different preloads and pivot offset. In both cases, copper backed pad material in the lower bearing half was examined for its superior heat dissipation characteristics.

The stability analysis was performed for the different bearing configurations by computing the damping ratio at the first critical speed. The unbalance response at the first critical speed and at running speed was also computed for all the different bearing configurations. Maximum bearing temperatures were also computed for center pivot and offset pivot pads, and also for different pad materials. The results confirmed the ability of the copper backed pads in providing lower temperatures and, thus, a higher degree of reliability.

The final bearing configurations for the #1 and #2 bearings are shown in Figures 10 and 11. The #1 bearing is a five pad bearing with a load-between-pad configuration. The #2 bearing is a four pad bearing, also with a load-between-pad configuration. Both bearings have a preload of 0.25 and copper pads in the bottom half of the bearing.

Field Balancing Simulation

The unit was balanced in March 1993, to reduce the synchronous vibrations. The data before and after adding the balance weights were documented, including the amount and location of the added weight. It was of interest to see if the rotordynamic model for the rotor-bearing system, as it existed then, could be simulated. The measured vibrations and the influence of the unbalance weight on the response were calculated. An unbalance weight of 117 oz-in was placed at the same plane

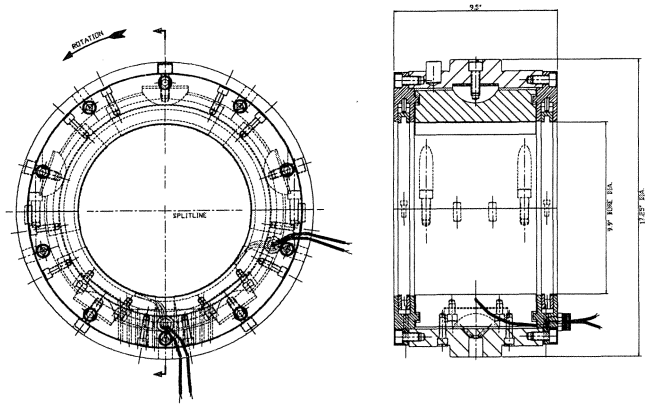

Figure 10. Self-Aligning Ball-in-Socket #1 Tilt Pad Bearing.

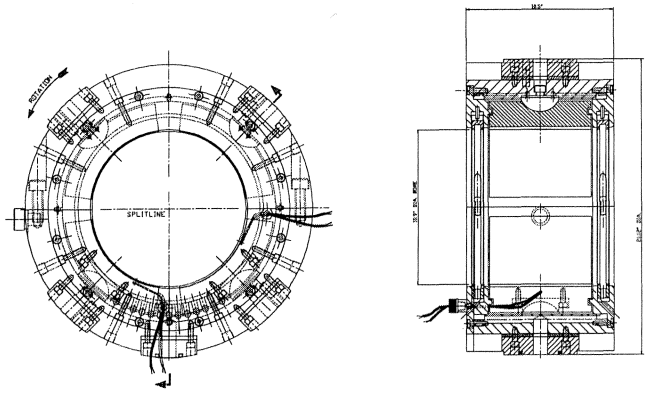

Figure 11. Self-Aligning Ball-in-Socket #2 Tilt Pad Bearing.

where the balancing took place in 1993. This was equivalent to 7 oz placed at a radius of 16.75 inches. The response with and without the weight is shown in Figure 12. The effect of this weight matched very well the effect introduced in the field balancing. The location of the balance plane was also very strategic for the mode of interest, as shown in the damped mode plot in Figure 13. The deflected rotor shape at operating speed, superimposed on the rotor model, is shown in Figure 14, and the balancing plane is indicated on the plot. The results of this analysis have also shown the influence of the overhung extension rotor/pump on the mode shape at operating speed.

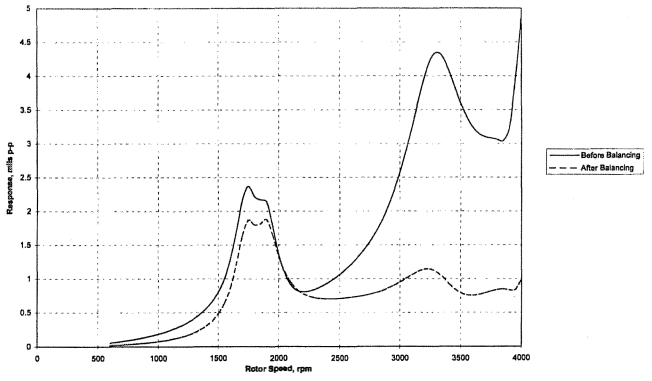

Figure 12. Response Simulation Before and After Balancing.

Steady Bearing Simulation

The extension rotor/pump represents a significant overhung mass that is mainly supported by the lube oil pump seals. The vibrations at the extension rotor can be very high and often results

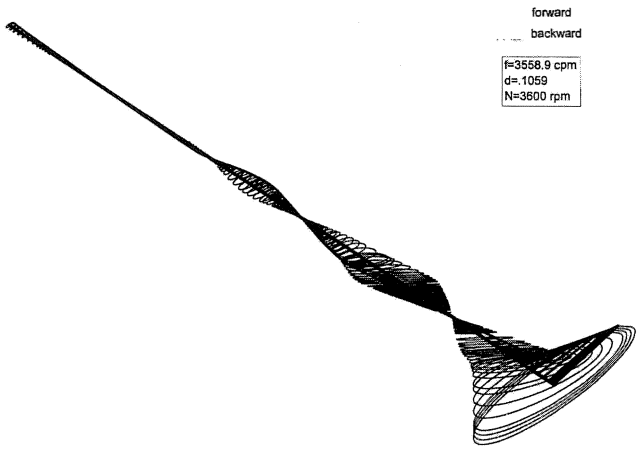

Figure 13. Mode Shape Corresponding to Eigenvalue at 3558.9 CPM.

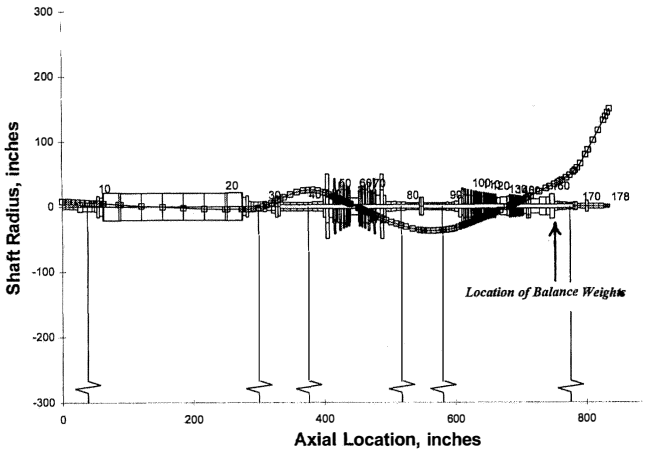

Figure 14. Deflected Rotor Shape at Operating Speed and Location of Unbalance Correction Plane.

in premature failure of the lube oil pump seals. It was of interest to investigate the benefits obtained from installing a steady bearing at this location. The rotor model with the steady bearing is shown in Figure 15. The response with and without the steady bearing at the #1 bearing location is shown in Figures 16 and 17, respectively. The response at the extension rotor, with and without the steady bearing, is shown in Figures 18 and 19, respectively. The steady bearing has a significant influence on the vibration levels and will extend the seal life for the lube oil pump. This simulation verified that the steady bearing modification would be beneficial for increased reliability of the unit.

MEASUREMENTS AFTER THE 1996 OUTAGE

Performance measurements were made after the outage to verify if the modifications achieved the desired goals. The unit efficiency was very good, as we were able to achieve the 120 MW load with only five of the six steam nozzles open. The unit did not experience any of the vibrations in the 90 to 100 MW range, which was a problem with the previous bearings. Vibrations peaked during cold starts in the 60 MW range and this characteristic was also present with the previous bearing configuration. Orbital data as a function of MW load indicated that the asymmetry in the bearing supports, when the load changed direction, was the major contributor to this phenomenon.

Measurements of Backward Whirl

The shaft orbit as measured by two eddy current probes placed 90 degrees apart (45 degrees on both sides of top dead center),

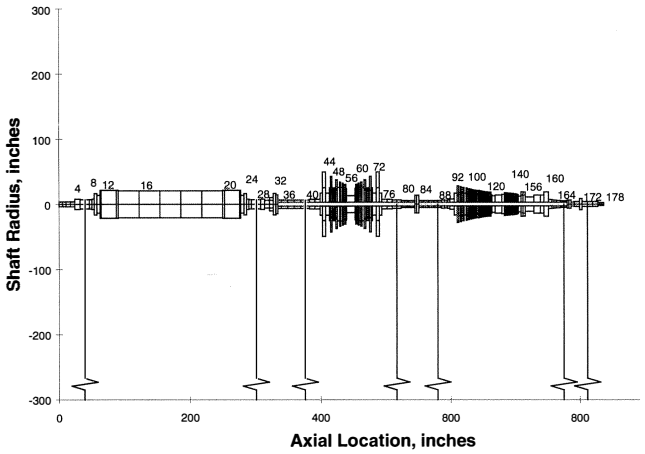

Figure 15. Rotor Model with Steady Bearing at Station #173.

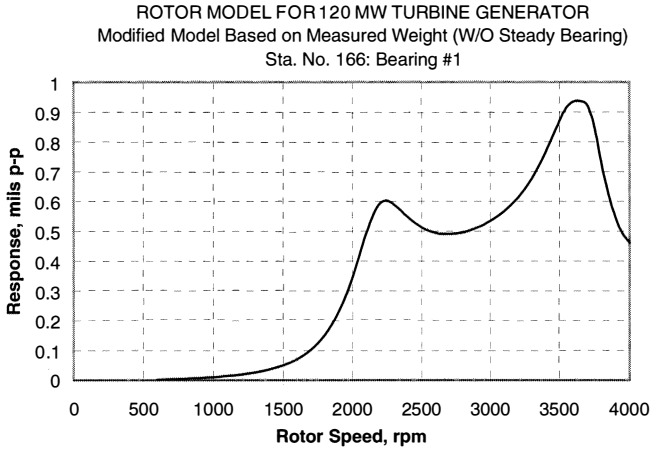

Figure 16. Response at Bearing #1 without Steady Bearing.

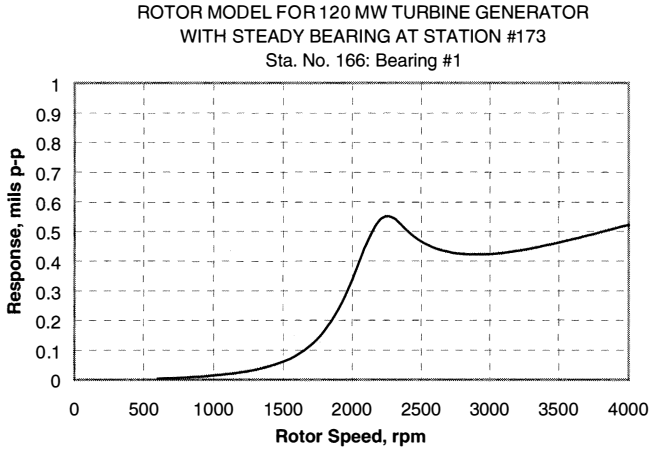

Figure 17. Response at Bearing #1 with Steady Bearing.

indicated that the rotor was undergoing backward whirl motion. In most conventional analysis where such a phenomenon is theoretically predicted to take place (Vance, 1988), the location of the running speed happens to fall between the horizontal and vertical critical speeds. In this case, the rotor is synchronized at 3600 rpm (60 Hz), but the load is changing. The change in load magnitude and direction, due to partial steam admission effects, will influence the operating eccentricity in the bearing and, subsequently, the stiffness asymmetry. Consequently, the location of the critical speeds will shift even though the speed is constant.

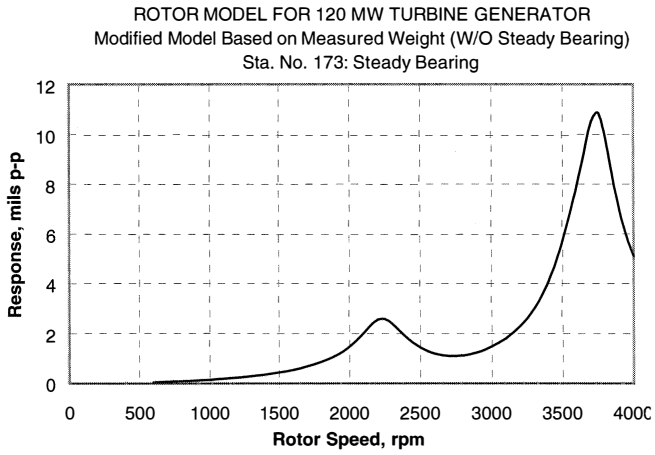

Figure 18. Response at Station #173 without Steady Bearing.

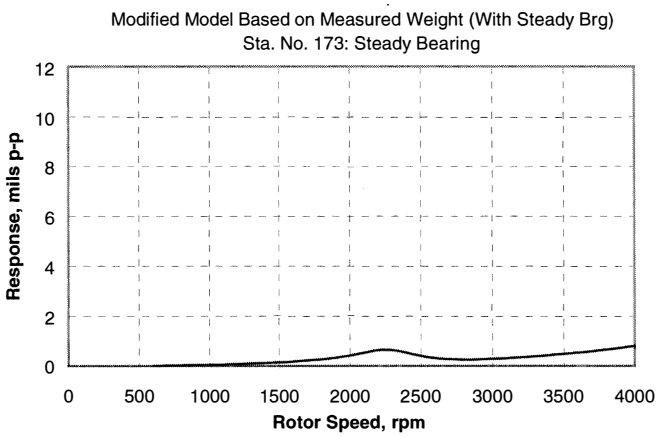

Figure 19. Response at Steady Bearing (Station #173).

As shown in Figure 20, the stiffness change caused the operating speed bearing stiffness to fall between the vertical and horizontal critical speed. This leads to the reverse or backward whirl in the range of 50 to 70 MW. At 54 and 60 MW, the rotor motion is almost a straight line, which is characteristic of the transition between forward and backward whirl. It is of interest to note here that due to the position of the eddy current probes at 45 degrees from top dead center (TDC), the vibration readings, as indicated by the probes, were much lower than the readings obtained with the shaft rider that was at TDC directly in line with the major axis of the vibration orbit.

The vibrations at this load (50 to 60 MW), where the transition takes place, is typically high when going through a cold start. In the case of a cold start, it is very likely that the rotor and stator may experience a rub condition due to thermal transients, as a result of differential expansion between the rotor and stator. Since the rotor is undergoing backward whirl due to the asymmetry in the stiffness, the occurrence of a rotor rub will intensify the backward whirl vibrations. This explains the higher vibrations measured during cold starts.

The backward whirl phenomenon is often dismissed as being theoretical or not physically possible. Recent awareness in rotordynamics and vibration instrumentation demonstrated that such a phenomenon is possible, and may exist in machines that have significant difference between the vertical and horizontal stiffness. In most cases, this difference is very small and the rotor usually passes through this zone too fast to allow the transient backward whirl conditions to subsist. In this case however, it was the load change that had a similar influence and shifted the

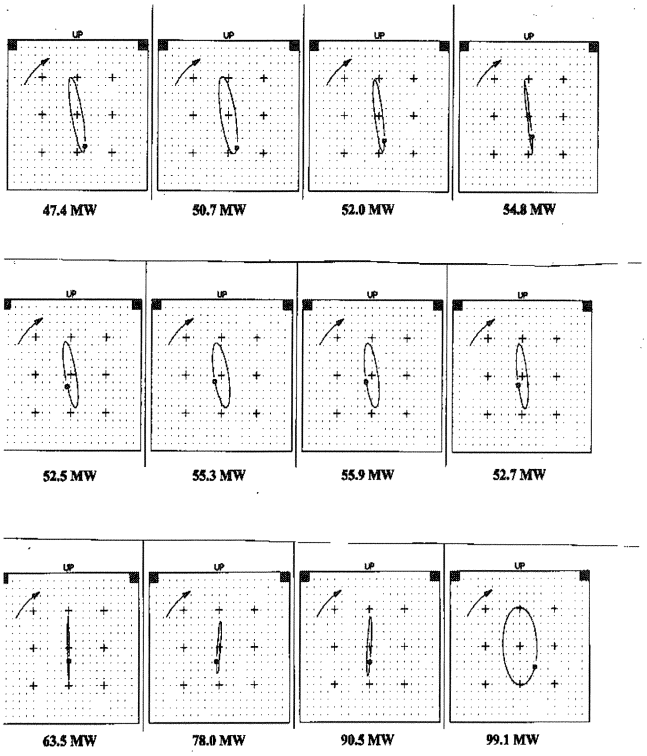

Figure 20. Bearing #1 Orbits Versus Load (0.1 mils/div).

higher stiffness critical speed (higher eigenvalue) down. Since the change in load was very gradual, it allowed us to capture this backward whirl phenomenon. In most other typical cases, the speed traversing the split critical, this would not have been possible.

Eccentricity Measurements

The installation of eddy current probes 90 degrees apart allowed measurements of the orbit plots shown above, in addition to shaft centerline eccentricity measurements. These are measurements of the DC gap voltage, which, when converted into mils, gives the shaft's centerline position within the bearing. This information was critical in determining the side loads due to bearing alignment and steam loading.

The shaft centerline movements versus speed/load for the #1, #2, #3, and #4 bearings are shown in Figure 21. The #3 bearing, being a sleeve bearing, will, as expected, cause the shaft to rise in the bearing as the speed increases and move to the left, due to the hydrodynamic cross-coupled stiffness. Since the #3 bearing is very close to the #2 bearing, it contributed to the side loading of the #2 bearing, as evidenced in bearing #2 shaft eccentricity movement. Four pad tilt pad bearings with load-between-pad configuration, such as that in the #2 bearing, should have very symmetric stiffness, and the shaft centerline, in the absence of side forces, should move straight up with speed. This side load to the left, and the fact that the shaft clockwise rotation will cause hot oil carryover from the lower right pad to the lower left pad, combined to make the left pad run about 196°F, while the right pad is at 165°F.

The #1 bearing centerline movement to the left was caused by the steam load. The improvements in efficiency allowed the unit to achieve the rated load of 120 MW, with only five of the steam valves open. With the sixth valve closed, as shown in the schematic in Figure 22, there would be a net side load pushing the rotor toward the left lower pad. This also resulted in differences in the two bottom pads' operating temperatures, similar to what was described for the #2 bearing above.

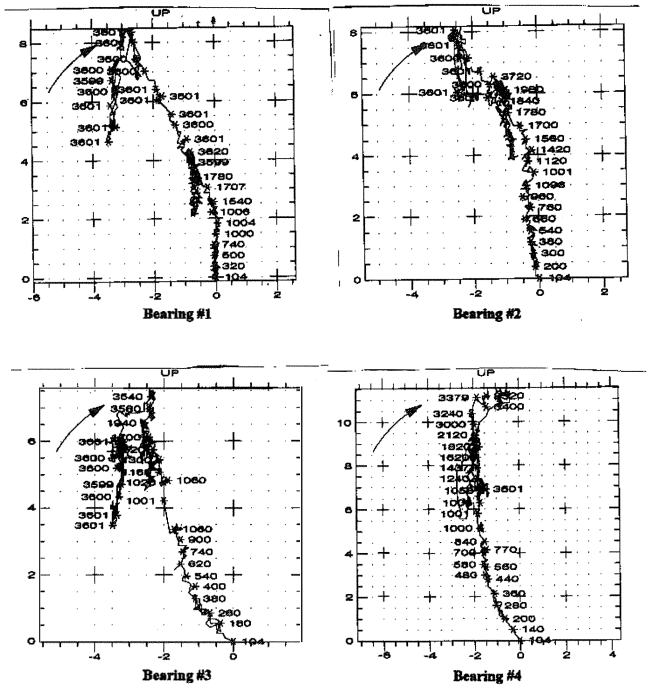

Figure 21. Shaft Centerline Position in Mils Versus Speed/Load.

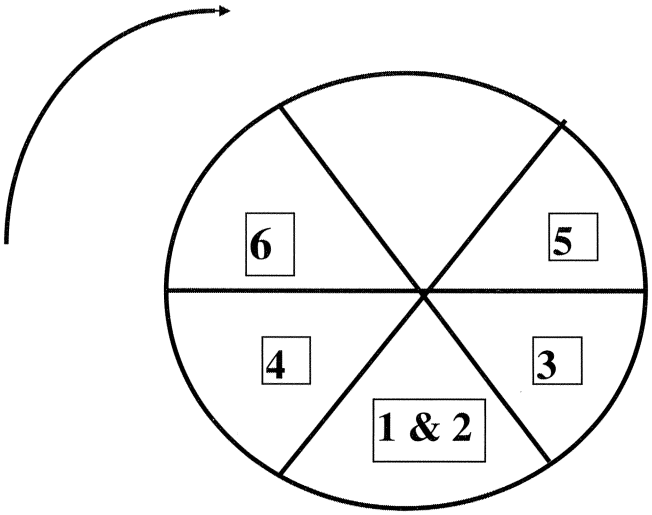

Figure 22. Steam Admission Valve Sequence.

SIMULATION OF BACKWARD WHIRL AND MEASURED ECCENTRICITY

The partial steam admission forced the rotor to load the pad on the left side of the bottom half. This condition was simulated to determine how this loading will influence the bearing temperature, which will be compounded with the hot oil carryover. The bearing dynamic coefficients will be markedly different from the load between pivot assumption, since, as evident by the eccentricity measurements, this will be closer to a load on pivot condition.

The dynamic coefficients at the specified eccentricity were also determined and input into the rotordynamic model. A split critical is evident in the response plot shown in Figure 23. A polar plot of this response is shown in Figure 24, and it clearly shows the split at 3600 rpm. The eigen analysis also verified the presence of a backward mode, as shown in Figure 25. The deflected rotor shape at operating speed, shown in Figure 26, also showed the influence of the backward mode on the response under these conditions of

load orientation. This is due to the fact that with the #5 nozzle fully open and the #6 nozzle closed, the resultant bearing load is on pivot. The bearing is very asymmetric, and the operating speed is just between the two split peaks. This is what caused the rotor to experience backward whirl at the load condition shown above, between 55 and 80 MW. Although backward whirl, by itself, is not of concern, the fact that it is present and coupled with a rub condition may intensify backward whirl vibrations. The conditions that helped create these were new tight clearance seals and the starting from cold conditions, where the rotor would expand at a higher rate than the casing.

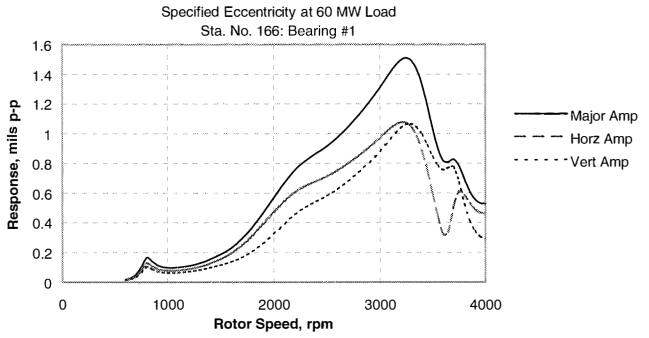

Figure 23. Unbalance Response Analysis Verifying the Split Critical at 3600 RPM.

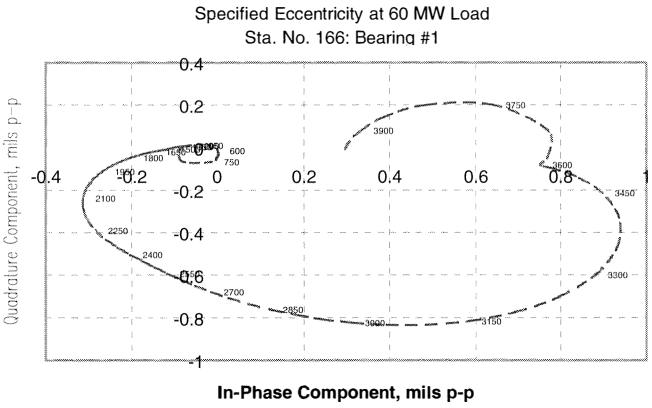

Figure 24. Polar Plot for the Response Showing the Split Critical at 3600 RPM.

CONCLUSIONS

The vibration measurements before and after the conversion provided great insight into the performance of the machine. This information highlighted characteristics and deficiencies that were addressed in the design and retrofit of the bearings. The shaft centerline measurements provided indications of the bearing alignment, steam loads, and the cross influence between adjacent bearings.

The vibration data were very critical in providing a benchmark for the rotordynamic analysis. The location of the critical speeds and influence of support stiffness were readily identified, ensuring that the bearing retrofit would eliminate some of the existing deficiencies without causing any adverse rotordynamic effects.

The measurements and identification of a stable backward whirl mode was of great interest from the academic and the practical point of view. This backward mode existed in the low MW range (50 to 60 MW), and therefore did not present a problem for this unit. It is important, however, to note that during cold starts, this range should be traversed with caution, since it will excite backward whirl

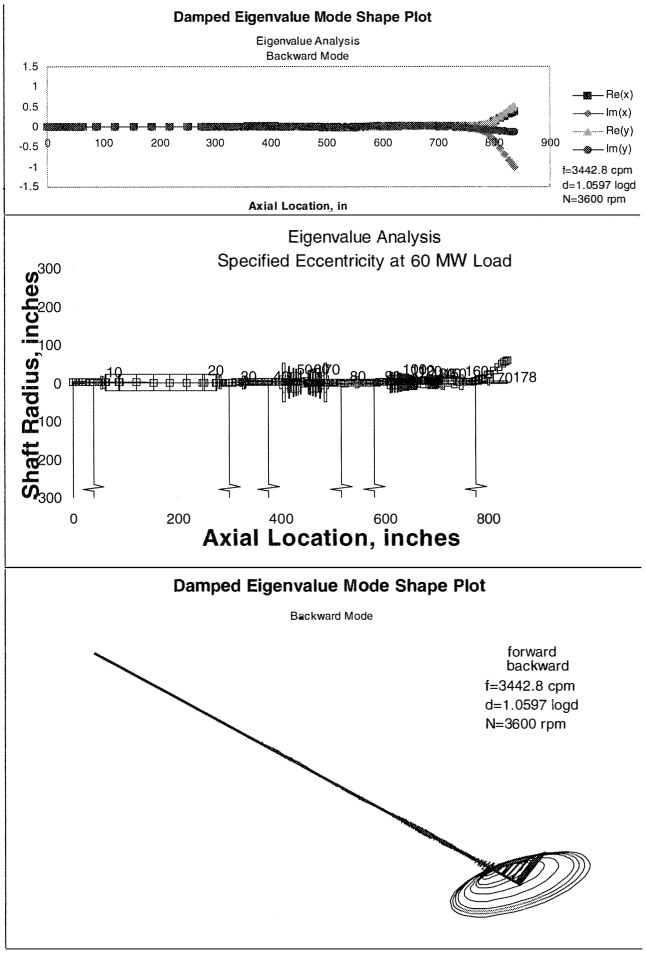

Figure 25. Eigen Analysis Predicting the Backward Mode.

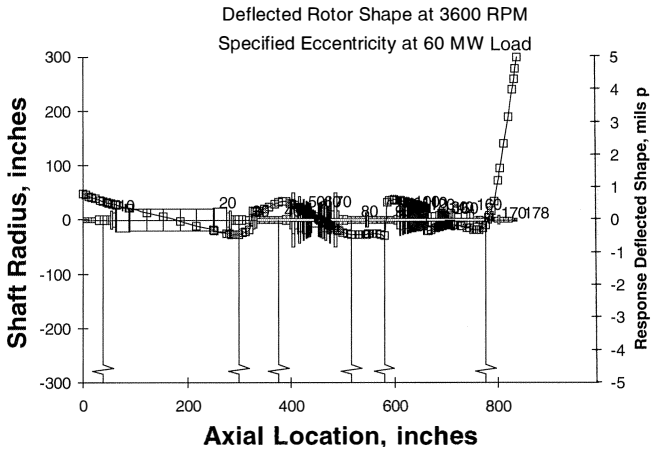

Figure 26. Deflected Rotor Shape.

during a rub condition. The location of the probes and the installation of two probes at 90 degrees (only one existed before the outage) allowed us to properly identify the presence of the backward whirl orbits. The orbit shape at 54 MW also presented an explanation for why the shaft rider located at TDC was reading much higher vibration than the eddy current probes located at 45 degrees on both sides of TDC. It also showed the limitations of existing vibration monitoring equipment that relies on just one probe or on two, but without the phase information. The major axis amplitude would have been more appropriate and would have provided a better picture and protection under these conditions.

REFERENCES

Gruwell, D. R. and Zeidan, F. Y., 1997, "The Use of Vibration Measurements in the Bearing Analysis and Retrofit of 120 MW Turbine Generator," ASME Joint Power Conference, Denver, Colorado.

Murphy, B. T., 1996-1998, XLROTOR, A windows based program for rotordynamic analyses. Rotating Machinery Analysis, Austin, Texas.

Vance, J. M., 1988, *Rotordynamics of Turbomachinery,* New York, New York: John Wiley & Sons.